

On the Asymptotic, Near-Equilibrium Sensory Response

Willy Wong*

*Department of Electrical and Computer Engineering, University of Toronto, Toronto M5S3G4 and
Institute of Biomaterials and Biomedical Engineering, University of Toronto, Toronto M5S3G9*

(Dated: April 25, 2022)

The asymptotic, near-equilibrium neural response of the sensory periphery can be derived exactly using information theory, asymptotic Bayesian statistics and a theory of complex systems. Almost no biological knowledge is required. The theoretical approach shows good agreement with experimental data across different sensory modalities and animal species. The theory is reminiscent of statistical physics.

PACS numbers: 87.19.lt, 02.50.-r, 87.19.lo, 87.18.-h

INTRODUCTION

Sensory transduction is the process whereby sensory stimuli are converted to neural responses. The sensory system is the gateway to the brain and transmitting information its most important task. The precise mathematical relationship between information and the peripheral sensory response is a topic of current interest.

This paper attempts to show that the asymptotic, near-equilibrium response of a peripheral sensory neuron can be characterized exactly using a single equation of information with no detailed knowledge of the underlying physiology. The basis of this approach is that the sensory system undergoes a measurement process involving the estimation of a sensory signal. The entropy of this estimate is then attributed to the response of the neuron. This is all that is required to understand the behaviour of a sensory neuron at its most elementary level.

The theory presented here concerns the problem of *intensity coding*. However, the methodology is general so that it can be applied to other types of biological information acquisition as well. Intensity coding is the process by which neurons encode information about the sensory stimulus strength. Increasing magnitudes of stimuli typically induce higher rates of response (in terms of action potentials per unit time). Also, the response of a neuron to a steady signal drops monotonically over time, a process known as adaptation.

This paper is a continuation of a series of papers detailing an information or entropy approach to sensory processing [1, 2]. From this theory, over 150 years of sensory science can be unified using a Boltzmann or Shannon measure of uncertainty together with a few auxiliary assumptions. This approach was later extended to neurophysiology [3, 4]. Despite the use of entropy, the exact connection to physics has not been thoroughly explored. This is the topic of the current paper where it is demonstrated that the asymptotic, near-equilibrium sensory response can be derived using ideas from information theory, asymptotic Bayesian estimation and complexity theory. There have been other studies which have looked at the coding of sensory information (e.g. [5–7]). But

generally they do not tackle the problem of responses in primary afferent neurons, and are considerably more complex than the approach presented here. Ultimately, the aim of this paper is to explore the generic principles of sensation and its relationship to physics.

DERIVATION OF MAIN EQUATION

Let θ denote the parameter estimated by the sensory system. In the case of intensity coding, θ refers to the magnitude of sensory stimulation. The sensory receptor draws repeated, independent samples X from an unknown distribution, i.e. $X_1, X_2, \dots, X_m \sim p(x|\theta)$. Given the prior distribution $\pi_0(\theta)$ (representing the uncertainty in θ before any measurements), after m samples the posterior distribution takes the form

$$\pi(\theta) = p(\theta|X_1, \dots, X_m) \propto p(X_1, \dots, X_m|\theta)\pi_0(\theta) \quad (1)$$

In the limit of large m , and under most conditions observed in nature, the posterior distribution is asymptotically normally distributed with mean parameter equal to the maximum likelihood value $\hat{\theta}$ and variance proportional to $\text{var}(X)/m$,

$$\pi(\theta) \xrightarrow{d} \mathcal{N}\left(\hat{\theta}, \text{var}(X)/m\right) \quad (2)$$

where $\text{var}(X)$ is the variance of the sensory signal. The form of the asymptotic distribution is independent of the choice of the prior. This result is discussed in greater detail below.

Stimulus samples are processed with limited resolution. We assume the error to be normally distributed with zero mean and variance R . The entropy is calculated from the mutual information obtained from the posterior and the error distributions. Taking the entropy of the convolution of the two distributions and subtracting the equivocation gives

$$H = \frac{1}{2} \log \left(1 + \frac{\text{var}(X)}{mR} \right) \quad (3)$$

This is simply the Shannon-Hartley law for an additive white Gaussian noise channel with signal-to-noise ratio equal to $\text{var}(X)/mR$ [8].

Equation (3) was first derived in the context of sensory processing over forty years ago [1]. The original derivation made use of the central limit theorem to derive the asymptotic form of the distribution of uncertainty in θ . In this paper, we use instead a Bayesian approach which makes clear the role of the prior distribution. The derivation of the posterior distribution in (2) requires a number of steps. Following [9], the asymptotic form of the posterior distribution for $m \rightarrow \infty$ can be shown to have mean equal to $\hat{\theta}$ and variance equal to the reciprocal of the Fisher information of θ . In the case where X belongs to the one-parameter exponential family (which includes most of the well-known random variables observed in nature) and θ is a natural parameter of the family, there exists an efficient estimator of θ which achieves the Cramér-Rao lower bound [10]. In this case, the reciprocal Fisher information equals $\text{var}(X)/m$. For the sensory problem considered here, θ is the signal magnitude, and the *sample mean* obtained from X_1, X_2, \dots, X_m is an efficient estimator of θ . Thus, implicit in this approach is the idea that the sensory receptor averages to estimate intensity.

By itself, (3) has already many of the characteristics required to describe mathematically the process of sensory transduction. Given a constant sensory signal, an increase in the number of samples or measurements results in a monotonic reduction of uncertainty H . Recall that during adaptation the sensory response to a steady input also falls monotonically. This suggests that entropy H can be related to the sensory response through the equation

$$F = kH \quad (4)$$

where F is the firing rate or spike response of a neuron and k is a positive constant with units of spikes per second. The fall in neural response during adaptation can be interpreted as a gain in certainty in the sensory signal. When the uncertainty vanishes, there is no response. The association of firing rate with uncertainty also permits the testing of theory with experimental data. For extensive discussion and the origins of this equation see [2].

The postulate in (4) fundamentally changes our view of sensation. At its core, this equation suggests that sensation quantifies *measurement uncertainty*. When (4) is combined with (3), we see that the peripheral neural response must increase monotonically with signal variability. Is this prediction supported by experimental observation? For example, the phenomenon of brightness enhancement (aka the Brücke-Bartley effect, e.g. [11]) shows that the apparent brightness of a flickering light can change with the frequency of flicker when time-average luminance is kept constant. However flickering

contributes to temporal variations in the signal resulting in the enhancement in apparent brightness. Other experiments involving the stabilization of an image on the retina show that prolonged exposure to a fixed image leads to the fading of the visual percept, e.g. [12]. In each case, we observe that the sensory response is coupled to variations in the signal. There are other theoretical approaches that postulate that sensation is coupled to variation or changes in the signal, e.g. [13, 14].

However, neither of the above experiments probe the exact relationship between variance and *firing rate*. Instead a new experimental test can be proposed to test this assumption directly. Light exhibits very different statistical behaviour depending on whether it is in the classical or quantum limit. Photon bunching is the phenomenon whereby the statistics of the photon count deviates from a Poisson distribution (e.g. [15]). If a photoreceptor is stimulated with such a signal, the resulting neural response can be recorded to test the dependency of firing rate on variance with mean held constant.

Yet it is clear that the neural response is related to the mean of the signal. An increase in mean generally results in an increase in neural response. As such, we expect the dependency of F to be on $E(X)$ and not $\text{var}(X)$. How can this discrepancy be resolved? Some recent work has shown that many complex systems exhibit a power-law relationship between mean and variance. The fluctuation scaling law was first discovered in ecology through animal population studies and is known also as Taylor's law [16]. A compelling explanation for the fluctuation scaling law was recently proposed [17]. The family of probability distributions known as the Tweedie distributions exhibits a power law relationship between the mean and variance. A convergence theorem has been established suggesting a reason for the ubiquity of the power law in complex systems [18].

Let us assume for now the applicability of the fluctuation scaling law to sensory signal statistics. Introducing $\text{var}(X) = \epsilon\mu^p$, where ϵ and p are positive constants and $\mu = E(X)$ and defining a new constant $\beta = \epsilon/R$, we obtain

$$H = \frac{1}{2} \log \left(1 + \frac{\beta\mu^p}{m} \right) \quad (5)$$

The response is now a monotonic increasing function of the mean. See [1] for the original derivation of this equation.

The signal mean consists of both external and internal sources. The external source is the sensory signal itself and any other external environmental signals. Internal sources may include other signals generated internally including thermal noise, self-generated signals, etc. We model the signal mean as a sum of the two components $\mu = I + \delta I$ where I is the total magnitude of external sources and δI the sum of internal sources. δI will generally be small relative to the external input for almost

the entire range of I .

Next we consider the role of time in the sensory response. Sample size increases with the number of measurements taken. Hence m is a function of time and dm/dt refers to the *sampling rate*. It is reasonable to assume that the sample size does not increase indefinitely: when the number of samples attains the optimal value, the sample size remains constant. Sampling is thus a function of the difference between the current sample size m and the optimal value m_{eq} . That is,

$$\frac{dm}{dt} = g(m - m_{eq}) \quad (6)$$

where g is some function with the condition $g(0) = 0$. Near equilibrium, we take a Taylor expansion around $m = m_{eq}$ to obtain

$$\frac{dm}{dt} \simeq g(0) + \dot{g}(0)(m - m_{eq}) \quad (7)$$

$$= -a(m - m_{eq}) \quad (8)$$

Since the number of samples m must be less than m_{eq} and $dm/dt \geq 0$, $a = -\dot{g}(0)$ is a positive time constant. Solutions of m are used to calculate H from (5) given a choice of m_{eq} .

One final step is required before the derivation is complete. The determination of an optimal sample size (m_{eq}) will depend on the precise condition for optimality. In the Appendix, it is shown that if the estimation error is constrained then the optimal sample size must grow as a function of stimulus intensity in the form

$$m_{eq} = (I + \delta I)^{p/2} \quad (9)$$

That is, the sample size must grow as a power function of intensity.

Summarizing, we have

$$F = kH \quad (10)$$

$$H = \frac{1}{2} \log \left(1 + \frac{\beta (I + \delta I)^p}{m} \right) \quad (11)$$

$$\frac{dm}{dt} = -a(m - m_{eq}) \quad (12)$$

$$m_{eq} = (I + \delta I)^{p/2} \quad (13)$$

As we will see, these equations give a good description of the neural response to most time-varying sensory inputs up to physiological saturation levels.

DISCUSSION

The derivation above requires the use of a Tweedie distribution with $\text{var}(X) = \epsilon E(X)^p$. Tweedie distributions belong to the exponential family. They exist for all real values of p except $0 < p < 1$ [18]. This turns out to have important consequences for the growth of the

neural function. Compression is an essential property of sensory neurons since sensory signals can range over several orders of magnitude while the dynamic range of a peripheral neuron is far more limited.

In the asymptotic limit of large sample size where $m = m_{eq}$, one can easily derive from Eqs. (10-13) the result

$$F = \frac{k\beta}{2} (I + \delta I)^{p/2} \quad (14)$$

A compressive response involves a power exponent less than one. Since p itself is positive, and no such Tweedie model exists for $0 < p < 1$, this implies that the only possible range of exponents lies within $p \in [1, 2)$. Such Tweedie models are known as *compound Poisson-gamma models* [18]. A compound Poisson-gamma model can be generated via a sum of gamma-distributed random variables, with the number of summed terms itself Poisson distributed.

Fluctuation scaling would thus imply that the interaction between signal and receptive field is well-characterized by a Poisson-gamma model when the response is compressed relative to the range of input. In the olfactory system, for example, odourant molecules bind with receptor sites on the cilia in the epithelial layer [19]. At steady-state, the number of binding events per unit interval of time is likely Poisson distributed. The number of receptor sites activated is a cluster and cluster sizes are often modelled by gamma distributions. It would appear that the Poisson-gamma model provides not only a reasonable model for olfaction, but for other modalities as well. For sensory modalities where the range of stimuli is more limited (e.g. mechanoreception or stretch sensing), the neural response may not necessarily be compressive. When $p > 2$, this would imply that X has a distribution belonging to the family of positive stable distributions [18].

PREDICTIVE SCOPE OF THEORY

Time-independent inputs

The equations governing sensory entropy can be solved for different inputs or experimental configurations. We will consider a number of examples involving piece-wise constant inputs. First consider the solution for a step input illustrated in Figure 1a. We divide the solution into three distinctive regions: Region I ($t < 0$) where the stimulus is off, II ($0 \leq t < t_0$) where stimulus is turned on, and III ($t \geq t_0$) where the stimulus is turned off.

Next the relevant response is solved assuming that the neuron is equilibrated (i.e. fully adapted) prior to $t < 0$. In this case the sample size $m(t)$ can be solved from (12)

and (13) to give

$$m_{\text{I}} = m_{eq1} \quad (15)$$

$$m_{\text{II}} = m_{\text{II}}(0)e^{-at} + m_{eq2}(1 - e^{-at}) \quad (16)$$

$$m_{\text{III}} = m_{\text{III}}(t_0)e^{-a(t-t_0)} + m_{eq3} \left[1 - e^{-a(t-t_0)} \right] \quad (17)$$

where $m_{eq1} = m_{eq3} = \delta I^{p/2}$ and $m_{eq2} = (I + \delta I)^{p/2}$. Continuity ensures that $m_{\text{II}}(0) = m_{\text{I}}(0)$ and $m_{\text{III}}(t_0) = m_{\text{II}}(t_0)$. Substituting m and I into (10)-(11) gives the response of the neuron F in all three regions. Other inputs (e.g. a double-step input in Figure 1b) can be solved similarly.

The challenge in evaluating (10)-(13) is to find experimental paradigms which allows for the robust determination of five unknown parameters. Unlike fundamental physics, these parameter values are not predetermined and are specific to receptor type, as well as to individual units. To avoid overfitting, we make use of the idea that multiple experiments conducted on the same unit should obey the same set of parameters. This is a stringent test of the theory as it greatly reduces the number of degrees of freedom allowed to the equations.

Next we compare theory with experimental data.

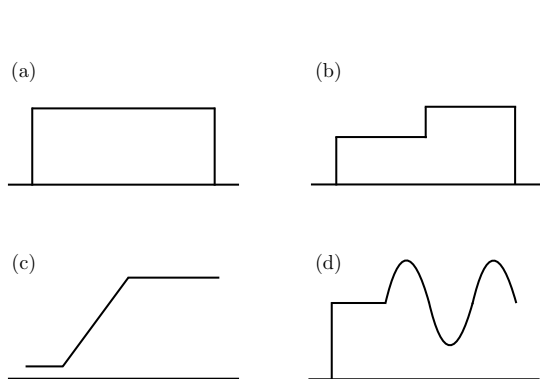


FIG. 1. A schematic illustration of sensory inputs commonly used to probe the response of sensory fibres. In all figures, the ordinate shows firing rate and the abscissa time. (a) A step input is used to measure adaptation. (b) Double-step function. (c) A ramp-and-hold stimulus. (d) Sinusoidally modulated intensity superimposed on a constant background.

Auditory adaptation and driven activity

Figure 2 shows data from two sources: an adaptation experiment (constant I , duration t is varied) and an intensity-rate experiment (constant t , I is varied) [20]. Data was recorded from the same auditory fibre of an anesthetized Mongolian gerbil (unit MB-52-11 from Figures 4 and 6). In the adaptation experiment, the number of spikes counted in a 960 μs interval was converted to a firing rate and observed as a function of time. An averaged firing rate was obtained over 91 trials. Figure 2a

(jagged line) shows the response to a 39 dB SPL tone presented at the characteristic frequency of the fibre (2.44 kHz). In the intensity-rate experiment, the maximal firing rate during a one millisecond interval was recorded as a function of different sound intensities. Figure 2b shows the intensity-rate response curve (open circles). After 40 dB, the response saturates and is not shown in Figure 2b.

The expression for F used to fit the data was derived from the sample size in Region II, i.e. (16), and is given by

$$F = \frac{1}{2}k \log \left[1 + \frac{\beta (I + \delta I)^p}{\delta I^{p/2} e^{-at} + (I + \delta I)^{p/2} (1 - e^{-at})} \right] \quad (18)$$

Since both experiments were conducted on the same auditory fibre, a common set of five parameters was used ($k = 1.3 \times 10^2$, $\beta = 2.2 \times 10^{-3}$, $p = 2.8$, $\delta I = 1.0 \times 10^{-4}$, and $a = 5.2$ Hz). Stimulus intensity in dB was calculated from rms pressure relative to 20 μPa . Figure 2 shows good compatibility between theory and data.

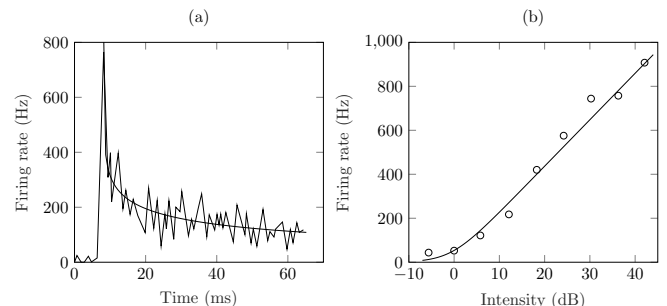


FIG. 2. Firing rate response recorded from the auditory fibre of a Mongolian gerbil [20]. Data in both figures recorded from the same fibre. Smooth curves show the predictions of (18) using a common set of parameters for both figures. (a) Firing rate measured as a function of sound duration for a 39 dB tone (jagged line). (b) Peak firing rate measured as a function of sound intensity in decibels (open circles).

Auditory double-step input

In [21], the response was measured to a series of double-step inputs from the auditory nerve of guinea pigs (data from Unit GP-6-2, see Figure 3 from original paper). A schematic illustration of the input is shown in Figure 1b. The initial response was elicited with a sound of intensity -4 , 2 , 8 , 14 , or 20 dB SPL followed by a 6 dB increase in the second pedestal. The solid line in Figure 3 shows the predictions with 5 adjustable parameters ($k = 1.3 \times 10^2$, $\beta = 6.7 \times 10^{-4}$, $p = 2.3$, $\delta I = 2.7 \times 10^{-7}$, $a = 2.6 \times 10^{-3}$ Hz). The match is not perfect although the

theoretical curves capture largely the behaviour observed physiologically (filled circles).

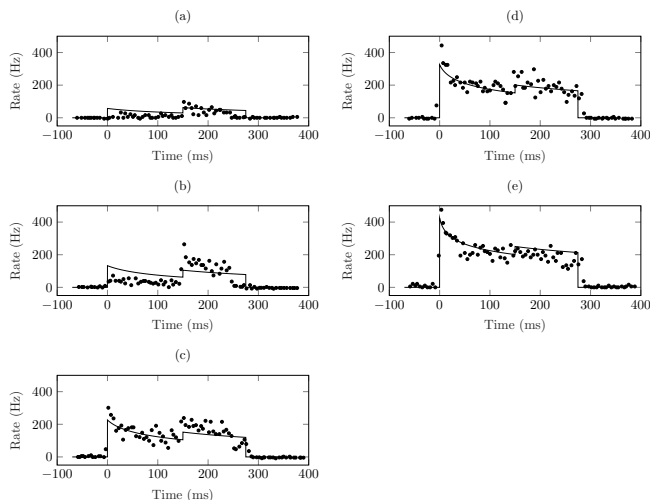


FIG. 3. Auditory neural responses measured from a double-step input in the guinea pig ear [21]. Initial pedestal with intensity $-4, 2, 8, 14$ or 20 dB, followed by a second pedestal 6 dB higher (panels a-e respectively). Firing rates indicated by closed circles. Smooth curves show the predictions of the equations solved for a double-step input using a common set of five parameters for all five graphs.

Peak versus steady-state response

In the same study, peak responses of the adaptation curve were compared to steady-state responses over a range of intensities (data of Unit GP-17-4 shown in Figure 1 of [21]). These results can be used to test a key component of the theory: that the optimal sample size grows with intensity following (9). In an attempt to reduce the number of parameters in (18), we approximate the equation by taking the large intensity limit. This is achieved by ignoring the ‘ $1+$ ’ term in (18) and taking internal noise to be small (i.e. $I \gg \delta I$) to obtain

$$F = \frac{1}{2}k \log \left[\frac{\beta I^p}{\delta I^{p/2} e^{-at} + I^{p/2} (1 - e^{-at})} \right] \quad (19)$$

The peak response is calculated by setting $t = 0$ and the steady-state response with $t \rightarrow \infty$:

$$F_{\text{peak}} = \frac{1}{2}k \log (\beta I^p) - \frac{1}{2}k \log (\delta I^{p/2}) \quad (20)$$

$$F_{\text{ss}} = \frac{1}{2}k \log (\beta I^{p/2}) \quad (21)$$

These two values, when plotted against the logarithm of intensity (or decibel), will yield two lines with slope differing by a factor of two. Figure 3 shows the predictions together with the experimental results from [21].

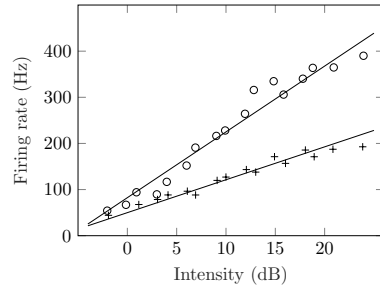


FIG. 4. Responses recorded from the guinea pig ear showing peak activity (open circles) and steady-state activity (crosses) from adaptation curves [21]. Solid lines show the predictions of the theory. The two lines are expected to differ by a factor of two in slope.

Multiple olfactory adaptation

The adaptation response in the sugar receptors of blowflies was measured for three different concentrations (0.01, 0.1 and 1 M, from Figure 4 of [22]). The experiment was conducted in the region where the adaptation was not fully complete. The concentrations are sufficiently high such that δI can be ignored. As such, we used a simpler version of (18) by taking $\delta I = 0$ and evaluating the first order Taylor series expansion for $t \ll 1/a$ in the denominator to obtain

$$F = \frac{1}{2}k \log \left[1 + \frac{\beta' I^{p/2}}{t} \right] \quad (22)$$

where $\beta' = \beta/a$.

This equation holds special significance as it is the original form of the equation governing sensory response. First published in 1977, it was the first attempt to use entropy to connect together various empirical sensory laws and appeared in a number of publications (e.g. [1, 2]). The simultaneous fit shown in Figure 5 was originally published in 1991 [23]. In total, 3 curves were fitted using 3 unknown parameters ($k = 1.1 \times 10^2$, $\beta' = 1.5 \times 10^3$ and $p = 1.3$).

Time-varying inputs

Hitherto, we have considered responses to inputs that are piece-wise constant. In general, analytical solutions for time-varying inputs are not possible due to the exponent in (9). However, numerical solutions can be easily obtained by either solving the differential equation in (12) using an Euler method or through numerical integration.

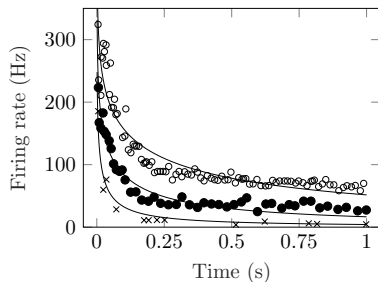


FIG. 5. Adaptation responses recorded in the sugar receptor of a blowfly for three concentrations (1.0 M open circles, 0.1 M filled circles, 0.01 M crosses) [22]. The responses were recorded from the same unit. Smooth curves indicate a simultaneous curve-fit with (22) using the same three parameters for all three data sets. Figure and result adapted from [23]

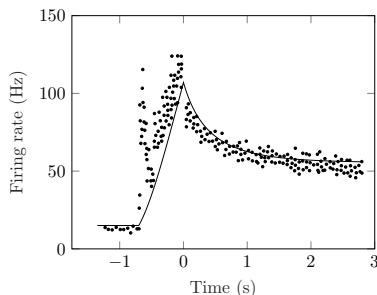


FIG. 6. Neural response to the ramp-and-hold lengthening of a cat muscle fibre [24]. The theoretical prediction requires a numerical solution to the differential equation in (12). In total, 4 parameters were used to fit three experimental regions: the initial steady-state region, ramp and subsequent adaptation response.

Muscle ramp-and-hold

In this example, the response of a cat muscle fibre was recorded to a ramp input (see Figure 1 of [24]). The fibre was elongated linearly and then held fixed at its final length. A schematic representation of the input is shown in Figure 1c. The stimulus in this case is a time-varying function. The solution for the sample size m was obtained by solving (12) numerically. In an attempt to reduce the number of parameters, the small intensity limit of (11) was adopted by taking the linear approximation $\log(1+x) \simeq x$. k and β combine to become a single parameter. In total, 4 parameters were used for 3 experimental regions ($k\beta = 0.23$, $\delta I = 3.0 \times 10^{-4}$, $p = 4.3$ and $a = 1.2$ Hz).

Sinusoidal variation and adaptation response in mechanoreception

Recordings were taken from the slit sense organ of a hunting spider [25]. Two different adaptation responses were recorded together with the response to a sinusoidal input from the same type of mechanoreceptor unit. (Both experiments were conducted on slit 2 of the lyriform organ although there is no indication of whether the recordings were made from the same receptor unit or not. See Figures 4 and 6 from original paper.) The mechanoreceptor responded only to the positive half of the sinusoidal input, which is typical for mechanoreception. Adaptation responses were calculated using (18) with inputs 0.0975° and 0.395° , while the sinusoidal input was evaluated through a numerical solution of (12) with a 0.38 Hz sinusoidal input with peak value 0.25° . Five parameters were used for three different experiments ($k = 31$, $\beta = 5.8$, $p = 6.1$, $\delta I = 6.6 \times 10^{-6}$ and $a = 1.8 \times 10^{-3}$ Hz).

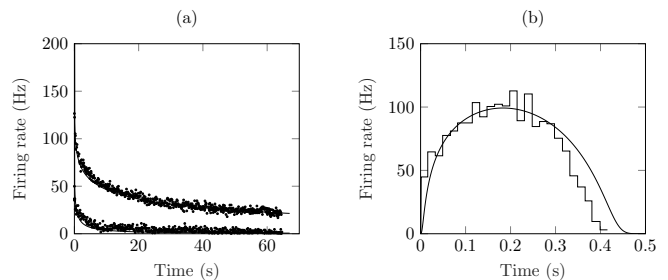


FIG. 7. Neural responses recorded from possibly the same mechanoreceptor unit of a hunting spider [25]. (a) Two adaptation responses to differing intensities (upper curve 0.395° , lower curve 0.0975°) together with predictions of (18). (b) Response to a 0.38 Hz sinusoidal input with peak deflection 0.25° (jagged line) with numerical solution of (10)-(13) (smooth line). A total of five adjustable parameters were used for all three experiments.

Square pulse versus sinusoidal responses in muscle spindle

The response of spindle afferents to repeated square pulse stimulation was compared to sinusoidal stimulation in the soleus muscle of cats (Figure 8 from [26]). The amplitude of the square pulses was matched to the amplitude of sinusoidal stimulation (following the usual definition of sinusoidal amplitude). The square pulse response in particular can be used to illustrate the mechanism of adaptation from a theoretical perspective. From (11) we see that firing rate is essentially a monotonic function of the ratio of intensity and sample size. Intensity can change abruptly but sample size always remain continuous. When the stimulus is turned on, the ratio

of I to m becomes large but falls as sample size grows to match the input (m approaches m_{eq}). At the termination of the input, the ratio falls to a small value before returning to steady-state values as sample size decreases to match the input. Such behaviour is typical of adaptation/de-adaptation responses and we observe it embedded mathematically within the equations.

In Figure 8 we show how parameters extracted from the square pulse response can be used to predict the response to sinusoidal stimulation. Adaptation responses can generally be characterized by three fixed points, the steady-state activity prior to the introduction of the stimulus F_{spon} , the peak firing rate F_{peak} and the steady-state activity F_{ss} associated with the input. These values can then be used to solve for the initial starting points or to constrain the fitting parameters used in the curve-fitting procedure. We extracted the three points by eye from Figure 8a: $F_{\text{spon}} = 24$ Hz, $F_{\text{peak}} = 41$ Hz and $F_{\text{ss}} = 32$ Hz. With one additional data point ($F = 34$ Hz at $t = 2.6$ s), all four parameters of the equation can be estimated to obtain the square pulse response ($k\beta = 9.8$, $p = 0.80$, $\delta I = 52$ and $a = 0.66$ Hz). From here, the same parameters were used to solve for the sinusoidal response shown in Figure 8b.

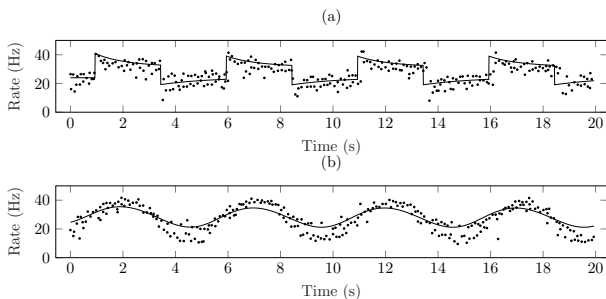


FIG. 8. The response of a cat muscle spindle to repeated stimulation [26]. (a) Response to square pulse stimulation compared to (b) sinusoidal stimulation. The amplitude for both inputs was identical ($50 \mu\text{m}$ stretch). Four parameters were used to predict both experiments from a numerical solution of (10)-(13).

Response amplitude as a function of modulation frequency in retinal ganglion cells

When light intensity is varied sinusoidally, the resulting neural response will be periodic. Figure 1d shows an example of a sinusoidally modulated input. The modulation depth is defined as $(I_{\text{max}} - I_{\text{min}}) / (I_{\text{max}} + I_{\text{min}})$. When this index is small, the equations can be solved analytically for an input of the form $I + \Delta I \sin(\omega t)$. The solution will have both a transient and a steady-state component. We are interested in the steady-state com-

ponent.

We begin by defining $Y = \Delta I / (I + \delta I)$. Y is equal to the modulation depth when $\delta I = 0$. In the limit of small Y , a linear expansion gives

$$F_{SS} = \frac{1}{2}k \log \left(1 + \beta (I + \delta I)^{p/2} \right) + kY C_1(I) C_2(\omega) \sin(\omega t + \phi) \quad (23)$$

where

$$C_1(I) = \frac{p}{2} \frac{\beta (I + \delta I)^{p/2}}{1 + \beta (I + \delta I)^{p/2}} \quad (24)$$

$$C_2(\omega) = \sqrt{\frac{1/4 + \omega^2/a^2}{1 + \omega^2/a^2}} \quad (25)$$

$$\phi = \arctan \left(\frac{\omega/a}{1 + 2\omega^2/a^2} \right) \quad (26)$$

Thus the steady-state response is itself sinusoidal.

Figure 9 shows the response of a cat retinal ganglion cell to sinusoidally modulated light (from Figure 9a of [27]). Response amplitude is defined as the difference between the highest and lowest firing rates, and was measured as a function of modulation frequency. Before comparing (23) to data, it is important to remember that the response of a single ganglion cell is determined from the input of many photoreceptor cells. Following [28], it has been shown that these individual photoreceptor inputs sum linearly. However, due to differences in path length and transduction time, a time jitter is introduced when these inputs are summed. By the central limit theorem, the jitter can be considered normally distributed. The amplitude of the average response from the ganglion cell is therefore convolved with a Gaussian kernel with zero mean and variance σ_{jitter}^2 . From here the average response amplitude can be calculated to be

$$2kY C_1(\omega) C_2(I) \exp(-\omega^2 \sigma_{\text{jitter}}^2 / 2) \quad (27)$$

Finally, the width of the time jitter can be shown to be related to the time constant of adaptation in the manner of $\sigma_{\text{jitter}} = 1/2a$ similar to the time-frequency bandwidth tradeoff [29]. Thus, response amplitude becomes

$$2kY C_1(\omega) C_2(I) \exp(-\omega^2 / 8a^2) \quad (28)$$

In the large intensity limit, this is an equation of four parameters which can be fitted to experimental data. In Figure 9 the response amplitude was measured to a signal with modulation depth 0.5 [27]. This violates the condition under which (23) was derived. Nevertheless, a comparison of theory to data is attempted. Since intensity is fixed, there are only two fitting parameters: one is the scaling factor for response amplitude, the other is a which scales the frequency axis. On a log-log plot, this amounts to a shift in the horizontal and vertical axes. Everything else is ‘locked in’ by the theory. Equation (28)

is plotted along side the data in Figure 9. The entire characteristic shape of the response curve is reproduced, including the inflection observed at low frequencies.

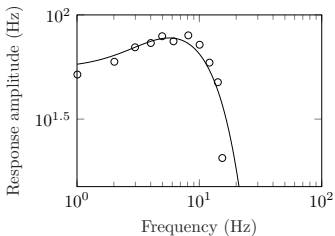


FIG. 9. Response amplitude of a cat retinal ganglion cell as a function of modulation frequency for a sinusoidally modulated input (open circles) [27]. The smooth curve was generated from the theory using only two scaling parameters. Please see text for more details.

FINAL REMARKS

The theory developed in this paper has a particular mathematical simplicity because we have restricted the analysis to the asymptotic, near-equilibrium limit. The situation is more difficult if we considered the non-equilibrium case (small m , far from m_{eq}). In such situations, the response may depend strongly on the prior distribution $\pi_0(\theta)$ from (1) or on the precise mathematical form of the sampling rate function dm/dt in (6). Despite this, we have shown that the equations hold enormous predictive power across all time scales, for almost all sensory modalities and different animal species.

There is however one fundamental result governing the sensory response that can be derived even when far from equilibrium. Using a basic theorem of information theory [8], we can write for the entropy of the posterior distribution

$$H(\theta|X_1, \dots, X_m) \leq H(\theta) \quad (29)$$

where $H(\theta)$ is the entropy of the prior distribution and $H(\theta|X_1, \dots, X_m)$ the entropy over the posterior distribution. That is, entropy decreases or remains constant with additional samples or measurements. Since $F = kH$ and $dm/dt \geq 0$, we have

$$dF/dt \leq 0 \quad (30)$$

Thus, with minimal assumptions, we have proved that the sensory response to a constant stimulus must, on average, decrease or remain constant. This inequality, together with the use of Boltzmann-Shannon entropy and $F = kH$ suggests a deeper connection between sensory processing and statistical physics.

ACKNOWLEDGEMENTS

This work was supported by a Discovery Grant from the Natural Sciences and Engineering Research Council of Canada (NSERC). The author is grateful for the many helpful discussions with Professors Kenneth Norwich and Manfredi Maggiore, and with those who have worked on the entropy theory in the past: Sheldon Opps, Suraya Figueiredo, Gerry Fung, Zoe Zhao, Bruno de Oliveira Floriano, Prathima Sundaram and Sai Vemula.

Appendix: The optimal sample size

The optimal sample size m_{eq} is the number of samples after which m no longer changes. Since the fluctuation scaling law posits that the variance of a signal increases with the magnitude of the signal, constant m_{eq} implies that the estimation error in the mean will increase when intensity is increased. On the other hand, if standard error $\sqrt{\sigma^2/m_{eq}}$ is held constant, m_{eq} will take the form

$$m_{eq} \propto (I + \delta I)^p \quad (31)$$

requiring sample size to change significantly with intensity.

Between these two extremes lies a third possibility. Consider the situation where the sensory system is presented with an input of intensity I_1 which is later changed to I_2 . Without loss of generality, assume that $I_2 > I_1$. At steady-state, the standard error of I_1 is SE_1 . Let the initial uncertainty in I_2 be $SE_{2,initial}$. Increasing the number of samples will cause this error to fall. How is the steady-state error in I_2 determined? Taking SE_2 to be the geometric average of the standard errors, we obtain

$$SE_2 = (SE_1 \times SE_{2,initial})^{1/2} \quad (32)$$

That is, the error in estimating I_2 is equal to the average of the steady-state error in I_1 and the initial uncertainty in I_2 .

To see what effect (32) has on the optimal sample size, let $m_2(0)$ be the initial sample size just after the change in intensity. Since m must remain continuous across the boundary we have $m_2(0) = m_{eq,1}$, where $m_{eq,1}$ is the optimal sample size for I_1 . This calculation assumes that steady-state is achieved prior to the change in intensity. From this, we conclude that the expression σ^2/m_{eq}^2 is invariant to changes in intensity. Thus the general relationship between optimal sample size and intensity is

$$m_{eq} = c(I + \delta I)^{p/2} \quad (33)$$

where c is a constant. For simplicity, c is set to unity as it can be incorporated into β in (11). Equation (33) is the expression for optimal sample size used in the theory and can be tested both indirectly and directly through experiments.

-
- * willy.wong@utoronto.ca
- [1] K. H. Norwich, *Bulletin of Mathematical Biology* **39**, 453 (1977).
 - [2] K. H. Norwich, *Information, Sensation, and Perception* (Academic Press San Diego, 1993).
 - [3] K. H. Norwich and W. Wong, *Mathematical Biosciences* **125**, 83 (1995).
 - [4] W. Wong, *On the Physics of Perception*, Ph.D. thesis, University of Toronto (1997).
 - [5] P. J. Drew and L. F. Abbott, *Journal of Neurophysiology* **96**, 826 (2006).
 - [6] Y. Aviel and W. Gerstner, *Physical Review E* **73**, 051908 (2006).
 - [7] M. Famulare and A. Fairhall, *Neural Computation* **22**, 581 (2010).
 - [8] T. M. Cover and J. A. Thomas, *Elements of Information Theory* (John Wiley & Sons, New York, 2012).
 - [9] L. M. Le Cam and G. L. Yang, *Asymptotics in Statistics: Some Basic Concepts* (Springer, 2000).
 - [10] K. A. Doksum and P. Bickel, *Mathematical Statistics: Basic Ideas and Selected Topics* (Prentice Hall, 2007).
 - [11] L. Marks, *Sensory Processes: The New Psychophysics* (Elsevier, 1974).
 - [12] F. Ratliff and L. A. Riggs, *Journal of Experimental Psychology* **40**, 687 (1950).
 - [13] D. Laming, *Sensory Analysis* (Cambridge University Press, Cambridge, 1986).
 - [14] L. Itti and P. Baldi, *Vision Research* **49**, 1295 (2009).
 - [15] H. Paul, *Reviews of Modern Physics* **54**, 1061 (1982).
 - [16] L. Taylor, *Nature* **189**, 732 (1961).
 - [17] W. S. Kendal and B. Jørgensen, *Physical Review E* **83**, 066115 (2011).
 - [18] B. Jørgensen, *The Theory of Dispersion Models* (Chapman & Hall, London, 1997).
 - [19] S. Pifferi, A. Menini, and T. Kurahashi, in *The Neurobiology of Olfaction*, edited by A. Menini (CRC Press, Boca Raton FL, USA, 2009) pp. 203–224.
 - [20] R. L. Smith, in *Auditory Function: Neurobiological Bases of Hearing*, edited by G. M. Edelman, W. E. Gall, and W. M. Cowan (John Wiley & Sons, Toronto, Canada, 1988) pp. 243–274.
 - [21] R. L. Smith and J. Zwislocki, *Biological Cybernetics* **17**, 169 (1975).
 - [22] V. Dethier and E. Bowdan, *Behavioral Neuroscience* **98**, 791 (1984).
 - [23] K. H. Norwich and K. M. V. McConville, *Journal of Comparative Physiology A* **168**, 151 (1991).
 - [24] S. Schäfer, *Experimental Brain Research* **102**, 198 (1994).
 - [25] J. Bohnenberger, *Journal of Comparative Physiology* **142**, 391 (1981).
 - [26] P. Matthews and R. Stein, *The Journal of Physiology* **200**, 723 (1969).
 - [27] B. Cleland and C. Enroth-Cugell, *Acta Physiologica Scandinavica* **68**, 365 (1966).
 - [28] C. Enroth-Cugell and J. G. Robson, *Journal of Physiology* **187**, 517 (1966).
 - [29] W. Wong, “Vision and sensory entropy,” (2019), in preparation.